Letter

Discovery of a Selective Phosphoinositide-3-Kinase (PI3K)-# Inhibitor (IPI-549) as an Immuno-Oncology Clinical Candidate

Catherine Anne Evans, Tao Liu, André Lescarbeau, Somarajan J. Nair, Louis Grenier, Johan André Pradeilles, Quentin Glenadel, Thomas Tibbitts, Ann M. Rowley, Jonathan P DiNitto, Erin E. Brophy, Erin L. O'Hearn, Janid A. Ali, David G. Winkler, Stanley I. Goldstein, Patrick O'Hearn, Christian M. Martin, Jennifer G. Hoyt, John R. Soglia, Culver Cheung, Melissa M. Pink, Jennifer L. Proctor, Vito J. Palombella, Martin R. Tremblay, and Alfredo C. Castro

ACS Med. Chem. Lett., **Just Accepted Manuscript** • DOI: 10.1021/acsmedchemlett.6b00238 • Publication Date (Web): 22 Jul 2016

Discovery of a Selective Phosphoinositide-3-Kinase (PI3K)-γ Inhibitor (IPI-549) as an Immuno-Oncology Clinical Candidate

Catherine A. Evans,* Tao Liu, André Lescarbeau, Somarajan J. Nair, Louis Grenier, Johan A. Pradeilles, Quentin Glenadel, Thomas Tibbitts, Ann M. Rowley,[‡] Jonathan P. DiNitto, Erin E. Brophy, Erin L. O'Hearn,[†] Janid A. Ali, David G. Winkler, Stanley I. Goldstein, Patrick O'Hearn, Christian M. Martin, Jennifer G. Hoyt, John R. Soglia, Culver Cheung, Melissa M. Pink, Jennifer L. Proctor, Vito J. Palombella,[§] Martin R. Tremblay, Alfredo C. Castro*

Infinity Pharmaceuticals, Inc. 784 Memorial Drive, Cambridge, Massachusetts 02139, United States

KEYWORDS: IPI-549, PI3K-gamma inhibitor, phosphoinositide-3-kinase, isoform selectivity, neutrophil migration, immuno-oncology

ABSTRACT: Optimization of isoquinolinone PI3K inhibitors led to the discovery of a potent inhibitor of PI3K-γ (**26** or IPI-549) with >100-fold selectivity over other lipid and protein kinases. IPI-549 demonstrates favorable pharmacokinetic properties and robust inhibition of PI3K-γ mediated neutrophil migration in vivo and is currently in Phase 1 clinical evaluation in subjects with advanced solid tumors.

Phosphoinositide-3-kinases (PI3Ks) belong to a family of signal transducing enzymes that mediate key cellular functions in cancer and immunity. The primary role of these lipid kinases entails catalysis of the phosphorylation of the inositol ring of membrane phosphoinositides, which then serve as sites for the activation of secondary messengers involved in the regulation of multiple biological processes, including cell growth, survival, differentiation, proliferation and migration. PI3Ks are divided into three classes (I, II, and III) based on substrate specificity, sequence homology, and types of regulatory subunits. Class I PI3Ks are further divided into two groups: Class IA, which includes PI3K-α, β, and δ, and Class IB, which contains only one member, PI3K-gamma (γ). While Class IA PI3Ks are predominantly activated by receptor tyrosine kinase signaling, PI3K-γ is activated primarily by G-protein coupled receptors.[1-6]

The PI3K-γ isoform is expressed in immune cells and has limited, if any, expression in normal or malignant epithelial cells and connective tissue cells.[7] Studies of PI3K-γ knockout mice show that PI3K-γ is important for cellular activation and migration in response to certain chemokines.[7-8] PI3K-γ signaling is particularly important for the function of myeloid cells, where it is downstream of G-protein coupled receptors (GPCRs) (e.g., chemokine receptors) and RAS.[7-9] In addition, PI3K-γ can be activated in response to tissue hypoxia in these cells.[10] A critical role for PI3K-γ in the unique myeloid-derived cells that constitute a key component of the immune-suppressive tumor microenvironment has also been demonstrated in PI3K-γ deletion and kinase-dead knock-in studies. For example, murine syngeneic tumors grow slower when transplanted into immune-competent mice where PI3K-γ is genetically inactivated.[9,10] This growth reduction is due to the abrogation of tumor-associated myeloid cells that are known to promote an immune-suppressive tumor microenvironment that permits tumor growth.[9-12] In addition, tumor-associated myeloid cells are postulated to support tumor regrowth after radiation or chemotherapy, and to enable metastatic spread.[13] These preclinical studies highlight a critical role for PI3K-γ in myeloid cell biology, and suggest that PI3K-γ inhibition in tumor-associated myeloid cells may be effective at preventing tumor growth in a variety of settings.

To test the hypothesis that pharmacological inhibition of PI3K-γ in tumor-associated myeloid cells could block their immune-suppressive function and lead to enhanced immune attack on tumor cells, a potent and selective synthetic small-molecule inhibitor of the PI3K-γ isoform was needed. Although inhibitors of PI3K-γ have been reported over the past decade, their selectivity for PI3K-γ over other PI3K isoforms or pharmacologic properties were until recently not suitable for assessment of inhibiting only PI3K-γ in vivo.[14-23] Hence, we set out to identify potent and selective inhibitors of PI3K-γ with desirable drug-like properties.

The *N*-phenyl 8-chloroisoquinolinone motif served as a possible scaffold to explore alternative hinge binding motifs that may provide unique interactions with PI3K-γ.[24] To this end, we assembled a focused collection of 8-chloroisoquinolinone analogs that could be readily synthesized having hinge binding motifs containing at least one hydrogen bond acceptor and 0-2 hydrogen bond donors. We screened this focused collection for their ability to inhibit PI3K-γ and PI3K-δ at physiological ATP concentrations (3 mM) and were pleasantly surprised to see that compounds **1** and **2** showed moderate selectivity for PI3K-γ over PI3K-δ (Table 1).

Table 1. Structure-activity relationship from hinge (R_1) and linker modifications (R_2).

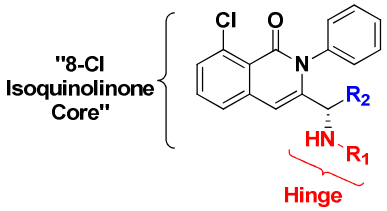

Cmpd	R_1	R_2	Biochemical IC_{50} (nM)[a]	
			PI3K-γ	PI3K-δ
1	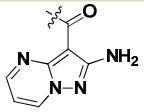	Me	40	400
2	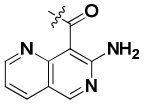	Me	60	320
3	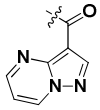	Me	400	800
4	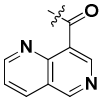	Me	1000	900
5	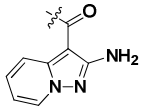	Me	300	2600
6	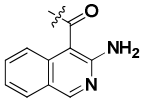	Me	>10000	>10000
7	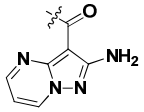	H	>7000	>10000
8	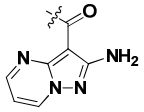	Et	150	600

[a] Data reported as the average of at least two runs. See Supporting Information for description of assay conditions and SEM values.

The hinge binding motifs on compounds **1** and **2** shared the following common features: an amide bond to isoquinolinone core with a chiral linker, an exocyclic amine as part of a hydrogen bond donor/acceptor pair, and a heterocyclic nitrogen oriented towards the core. The importance of these structural features on potency and selectivity was confirmed by a set of direct analogs of **1** and **2** (Table 1). Analogs without the exocyclic amine (**3** and **4)** were significantly less potent and selective than **1** and **2**, respectively. The carbo-analog of the 6-5 bicyclic system (**5**) was less active than the aza-analog (**1**), whereas the same modification on the 6-6 bicyclic system (**6** vs **2**) rendered the compound largely inactive against both PI3K isoforms. These data suggest that the dihedral angle between the carbonyl amide and the heterocyclic hinge binding motif **1** and **2** provides a preferred conformation for binding to both PI3K-γ and PI3K-δ. Changes to the chiral linker between the hinge binding motif and *N*-phenyl 8-chloroisoquinolinone core also proved to be deleterious to PI3K potency and selectivity. The enantiomer of **1** and the des-methyl achiral analog **7** were largely inactive against both PI3K isoforms. Interestingly, the selectivity was reduced when the chiral methyl is extended to an ethyl substituent (**8** vs **1**). These data highlight key hydrogen bonding features on the hinge binding motifs and the preferred chiral linker of *N*-phenyl 8-chloroisoquinolinones **1** and **2** that make them bona fide leads for the development of selective PI3K-γ inhibitors.

We evaluated leads **1** and **2** for selectivity across other PI3K isoforms and found **1** to be remarkably selective across other Class I and Class II PI3K isoforms (Table S1). Therefore, we focused our attention on further optimization of compound **1**. Taking the published co-crystal structures of propeller-shaped ligand PIK-39 with PI3K-δ and PI3K-γ into consideration, we evaluated C8 substitution on compound **1** to access a non-conserved region within PI3Ks with the aim of improving the PI3K-γ potency and selectivity (Table 2).[25, 26] We found small C8 substitutions such as methyl (**9**) and fluoro (**10**) did not have a profound impact on PI3K-γ potency or selectivity. However, a significant loss in PI3K-γ potency was seen with an electron-withdrawing cyano group (**11**) or electron-donating groups (**12-14**) at the 8 position. Vinyl substitution at the 8 position (**15**) also had a negative impact on PI3K-γ potency. However, 8-alkyne substitutions (**16** and **17**) unexpectedly provided modest improvements in potency for PI3K-γ over the 8-chloro substitution in **1**. Importantly, the methyl alkyne analog **17** also demonstrated weaker activity against PI3K-δ compared to **1** and **16**, and thus **17** had >40-fold selectivity for PI3K-γ over PI3K-δ, suggesting that the alkyne substitution makes significant non-favorable interactions with PI3K-δ at the non-conserved residues adjacent to the specificity pocket (Lys802 for PI3K-γ versus Thr750 for PI3K-δ) as does the aminopyrazolopyrimidine at the hinge binding region[21,22] (see Supporting Information, Figure S1).

Various substituted alkyne analogs at the 8-position that extended further into the non-conserved pocket were then prepared and evaluated for PI3K-γ potency and selectivity (Table 3). Additionally, as alkyl substituted alkyne analogs **16** and **17** suffered from poor in vitro metabolic stability, we also screened these substituted alkyne analogs for improved stability in mouse hepatocytes. Interestingly, hydrophobic substituents that extended deeper into the pocket (e.g. phenyl analog **18** vs. methyl

Table 2. Structure activity relationship of C8 substitution.

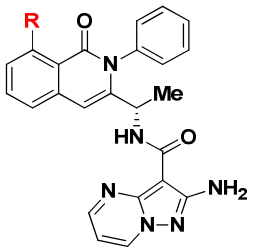

Cmpd	R	Biochemical IC_{50} (nM)[a]	
		PI3K-γ	PI3K-δ
9	Me	110	2600

10	F	50	530
11	CN	240	3100
12	OMe	1000	>9000
13	NHMe	1100	>10000
14	NMe_2	1100	>10000
15		330[b]	>10000
16		14	700
17		25	>1000

[a] Data reported as the average of at least two runs. [b]n=1. See Supporting Information for description of assay conditions and SEM values.

analog **17**) were found to have eroded PI3K-γ potency and selectivity. Less hydrophobic groups (e.g. pyridyl analogs **19-21**) maintained good selectivity for PI3K-γ and were found to be more metabolically stable than methyl alkyne analog **17**. With this in mind, we synthesized and evaluated various analogs with smaller heterocycles on the end of the 8-alkyne (e.g. **22-26**). Amongst various 5-membered ring heterocycle analogs, *N*-methylpyrazole analog **26** proved to have excellent potency and selectivity for PI3K-γ over PI3K-δ in enzymatic assays and excellent in vitro metabolic stability. Having achieved this remarkable selectivity in biochemical assays and in vitro metabolic stability, we further profiled compound **26** in various in vitro and in vivo settings.

Compound **26** was evaluated for activity across all Class I PI3K isoforms. The binding affinity of compound **26** for PI3K-γ was determined by measuring the individual rates constants (k_{off} and k_{on}) and for PI3K-α, β and δ using equilibrium fluorescent titration. Compound **26** was found to be a remarkably tight binder to PI3K-γ with a K_d of 290 pM and >58-fold weaker affinity for other Class I PI3K isoforms (Table 4). Additionally, compound **26** did not significantly inhibit a panel of 468 mutant and non-mutant protein and lipid kinases (including Class II PI3K isoforms) at 1 μM (Tables S1 and S4). In PI3K-α, -β, -γ, and -δ dependent cellular phospho-AKT assays, compound **26** demonstrated excellent PI3K-γ potency (IC_{50} = 1.2 nM) and selectivity against other Class I PI3K isoforms (>146-fold). Furthermore, compound **26** dose dependently inhibited PI3K-γ dependent bone marrow-derived macrophage (BMDM) migration in vitro (Figure 1).[28]

Table 3. Structure-activity relationship of C-8 alkynyl substitution.

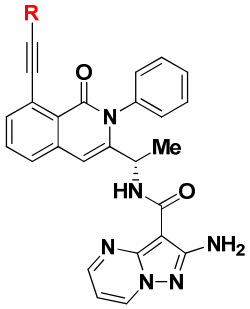

Cmpd	R	Biochemical IC_{50} (nM)[a]		Mouse Hepatocyte Stability $t_{1/2}$ (min)
		PI3K-γ	PI3K-δ	
18		280	140	ND
19		110	>6000	102
20	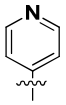	350	>9000	51
21	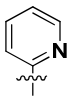	170	>9600	72
22		110	>8000	43
23		75	4800	270
24		360	>10000	27
25	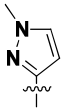	100	>9000	251
26	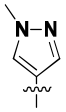	16	>8400	>360

[a] Data reported as the average of at least two runs. See Supporting Information for description of assay conditions and SEM values.

Table 4. Class I PI3K selectivity profile for compound 26 in biochemical and cellular assays.

Assay	PI3K Isoform			
	α	β	γ	δ
K_d (nM)[a]	17	82	0.29	23
Biochemical IC_{50} (nM)	3200	3500	16	>8400

Cellular IC_{50} (nM)[b]	250	240	1.2	180

[a] Binding affinities (K_d) of **26** were determined by methods previously reported.[24] See Supporting Information for full details.
[b] Cellular IC_{50}s for Class I PI3K-α, PI3K-β, PI3K-γ, PI3K-δ were determined in SKOV-3, 786-O, RAW 264.7, and RAJI cells, respectively, by monitoring inhibition of pAKT S473 by ELISA.

Compound **26** was also found to be selective against a panel of 80 GPCRs, ion channels, and transporters at 10 μM (see Supporting Information, Table S5 for full selectivity details). Additional in vitro safety assessment of compound **26** demonstrated that it was negative in Ames mutagenicity assays and had an IC_{50} greater than 10 μM in a hERG binding assay (data not shown).

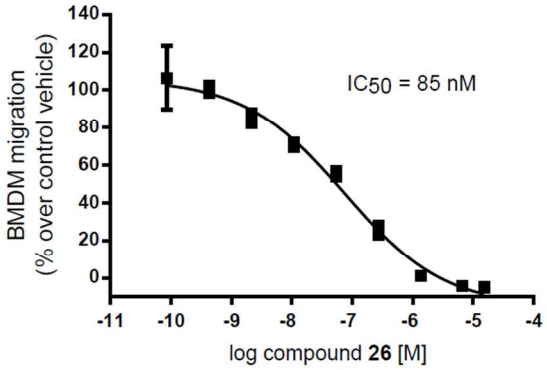

Figure 1. Effect of compound **26** on migration of bone marrow derived macrophages (BMDM) in vitro. BMDMs were stimulated to migrate toward 100 μg/mL CXCL12 (SDF-1α) for 3 hours through a 5 micron Boyden Chamber with or without DMSO or a dose response of compound **26**. Migrated BMDMs were counted and compared to control.

In vitro absorption, distribution, metabolism and excretion (ADME) properties and pharmacokinetic parameters of compound **26** were also determined (summarized in Table 5). In vitro, **26** showed moderate to high cell permeability across Caco-2 cell monolayers, was slowly metabolized in cultured hepatocytes ($t_{1/2}$ >360 minutes), and demonstrated IC_{50}s greater than 20 μM for the CYP isoforms tested (1A2, 2B6, 2C8, 2C9, 2C19, 2D6, 3A4). In vivo (mice, rats, dog, and monkeys), compound **26** had excellent oral bioavailability, low clearance, and distributed into tissues with a mean volume of distribution of 1.2 L/kg (Table 5). Overall, compound **26** had a favorable pharmacokinetic profile to allow potent and selective inhibition of PI3K-γ in vivo.

Based on the pharmacokinetic properties in mice and pharmacological in vitro profile, compound **26** was well-suited to investigate the impact of potent and selective PI3K-γ inhibition in vivo. IL-8 stimulated neutrophil migration into air pouches in mice has previously been shown to be dependent on PI3K-γ. Thus, to demonstrate PI3K-γ dependent activity of compound **26** in vivo, we evaluated the effect of orally administered compound **26** on IL-8 stimulated neutrophil influx into the air pouches on mice.[7,8] Compound **26** significantly reduced neutrophil migration in a dose dependent manner in this model when administered orally at all of the tested doses (Figure 2a). The degree of inhibition observed directly correlated with plasma concentrations of compound **26** in these mice (Figure 2b), clearly demonstrated that orally administered compound **26** can inhibit PI3K-γ function in vivo. In addition, compound **26** (IPI-549) has been shown to inhibit tumor growth in murine syngeneic models through alteration of immune cells in the tumor microenvironment.[28]

On the basis of its remarkable PI3K-γ potency and selectivity, favorable in vitro safety and pharmacokinetic profiles, and ability to inhibit PI3K-γ in vivo, compound **26** (IPI-549) was chosen as a development candidate. IPI-549 is currently in Phase 1 clinical evaluation in subjects with advanced solid tumors.[29]

Table 5. In vitro ADME and pharmacokinetics for compound 26.

In vitro ADME				
Caco-2 (P_{app} 10^{-6} cm/sec; A to B @ 10 μM)	13			
PPB (% free; mouse, rat, dog, monkey, human @ 1 μM)	2.2, 2.8, 2.8, 4.0, 1.1			
Metabolic stability ($t_{1/2}$; min)[a]	> 360			
CYP3A4 inhibition (IC_{50}; μM)	> 20			
Pharmacokinetics				
	Mouse	**Rat**	**Dog**	**Monkey**
C_{max} (μM)[b]	3.6	2.0	1.9	0.56
$AUC_{0-\infty}$ (ng*h/mL)[b]	20568	8049	1066	4030
$t_{1/2}$ (h)[c]	3.2	4.4	6.7	4.3
CL (mL/min/kg)[c]	3.6	4.4	2.8	4.3
V_{ss} (L/kg)[c]	0.8	1.2	1.3	1.3
%F	88	57	65	31

[a] Study conducted using cultured human hepatocytes.
[b] Determined from oral dosing to male animals; PO dose levels: 5 mg/kg mouse and rat, 2.5 mg/kg monkey and dog. Formulation; 0.5% Carboxymethylcellulose, 0.05% Tween80
[c] Determined from intravenous dosing to male animals: IV dose levels: 1 mg/kg mouse and rat, 0.5 mg/kg monkey and dog. Formulation; 5% NMP, 40% PEG400, 55% PBS

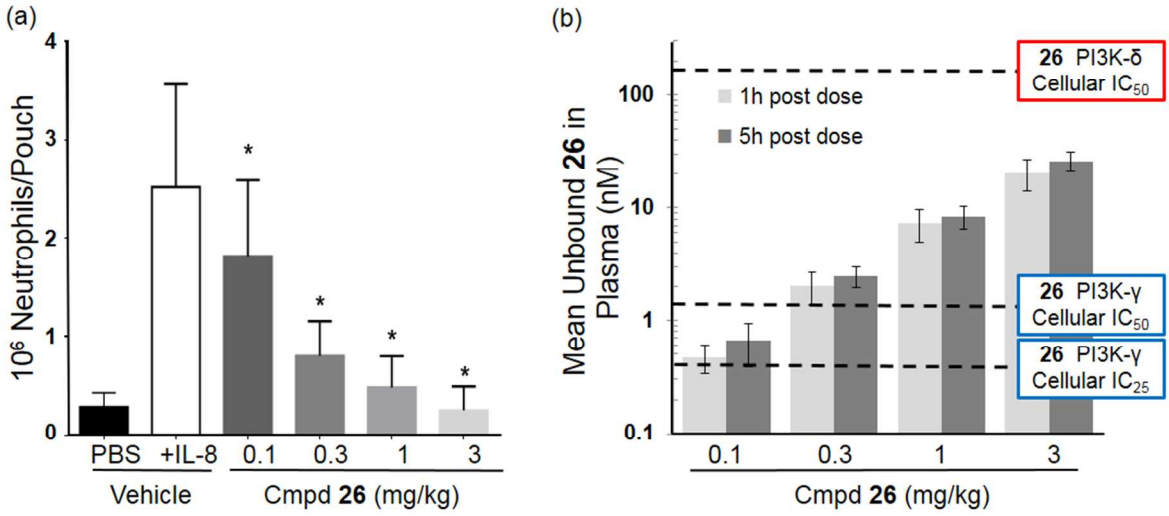

Figure 2. (a) Effect of compound **26** on neutrophil migration in the mouse air pouch model. Mice were dosed orally one hour before IL-8 was applied to the air pouch. After 4 hours the air pouch was lavaged and the neutrophils counted using a CELL-DYN hematology analyzer. *indicates p values <0.05 compared to vehicle. Error bars indicate the standard error of the mean of 10 mice per group. (b) Plasma concentration levels of compound **26** at 1 h and 5 h post administration with overlaying cellular IC_{50} (PI3K-γ and PI3K-δ) and IC_{25} (PI3K-γ) values.

ASSOCIATED CONTENT

Supporting Information

The Supporting Information is available free of charge on the ACS Publications website at DOI: XXX

Synthetic procedures and analytical data for **1**-**26**; PI3K biochemical and cellular assay conditions; PI3K Class I & II selectivity data for **1** and **2**; full selectivity data for **26**; general animal study protocols (PDF)

AUTHOR INFORMATION

Corresponding Authors

* E-mail: catherine.evans@infi.com
* E-mail: alfredo.castro@infi.com

Present Addresses

† Blueprint Medicines, Cambridge, Massachusetts 02139
‡ AbbVie, North Chicago, Illinois 60064
§ Surface Oncology, Cambridge, Massachusetts 02142

Notes

The authors declare no competing financial interest.

ACKNOWLEDGMENT

We thank Dr. Nicole Hurst for coordinating the preclinical safety evaluation of IPI-549, Dan Snyder and Amael Madec for assistance in preparation of early analogs, Drs. Jeff Kutok and Karen McGovern for guidance on the pharmacological assessment of IPI-549, and colleagues at Intellikine, Drs. Pingda Ren and Liansheng Li for their insights on PI3K inhibitors.

ABBREVIATIONS

ADME, absorption, distribution, metabolism , and excretion; AKT, protein kinase B; ADP, adenosine diphosphate; ATP, adenosine triphosphate; BMDMs, bone marrow-derived macrophages; CXCL12, chemokine C-X-C motif 12; CYP, cytochrome P450; DMSO, dimethysulfoxide; ELISA, enzyme-linked immunosorbent assay; GPCR, G-protein-coupled receptor; IL-8, interleukin 8; NMP, *N*-methyl-2-pyrrolidone; PBS, phosphate-buffered saline; PI3K, phosphoinositide 3-kinase; PPB, plasma protein binding; PEG, polyethylene glycol; SDF-1, stromal cell-derived factor 1

REFERENCES

(1) Cantley, L.C. The phosphoinositide 3-kinase pathway. *Science*, **2002**, *296*, 1655-1657.
(2) Vanhaesenbroeck, B.; Whitehead, M. A.; Pineiro, R. Molecules in medicine mini-review: isoforms of PI3K in biology and disease *J. Mol. Med*. **2016**, *94*, 5-11.
(3) Hawkins, P. T.; Stephens, L. R.; PI3K signaling in inflammation. *Biochim. Biophys. Acta, Mol. Cell Biol. Lipids* **2015**, *1851*, 882-897.
(4) Thorpe, L. M.; Yuzugullu H.; Zhao, J. J. PI3K in cancer: divergent roles of isoforms, modes of activation and therapeutic targeting. *Nat. Rev. Cancer* **2015**, *15*, 7-24.
(5) Rommel, C.; Camps, M.; Ji, H. PI3Kδ and PI3Kγ: partners in crime in inflammation in rheumatoid arthritis and beyond? *Nat. Rev. Immunol*. **2007**, *7*, 191-201.
(6) Banham-Hall, E.; Clatworthy, M. R.; Okkenhaug, K. The therapeutic potential for PI3K inhibitors in autoimmune and rheumatic diseases. *Open Rheumatol. J*. **2012**, *6*, 245-258.
(7) Sasaki, T.; Irie-Sasaki, U.; Jones, R. G.; Oliveira-do-Santos, A. J.; Stanford, W. L.; Bolon, B.; Wakeham, A.; Itie, A.; Bouchard, D.; Kozieradzki, I.; Joza, N.; Mak, T. W.; Ohashi, P. S.; Suzuki, A.; Penninger, J. M. Function of PI3Kγ in thymocyte development, T cell activation, and neutrophil migration. *Science* **2000**, *287*, 1040-1046.
(8) Hirsch, E.; Katanaev, V. L.; Garlanda, C.; Azzolino, O.; Pirola, L.; Silengo, L.; Sozani, S.; Mantovani, A.; Altruda, F.; Wymann, M. P. Central role for G protein-coupled phosphoinositide 3-kinase in inflammation. *Science* **2000**, 1049-1053.
(9) Schmid, M. C.; Avraamides, C. J.; Dippold, H. C.; Franco, I.; Foubert, P.; Ellies, L. G.; Acevedo, L. M.; Manglicmot, J. R. E.; Song, X.; Wrasidlo, W.; Blair, S. L.; Ginsberg, M. H.; Cheresh, D. A.; Hirsch, E.; Field, S. J.; Varner, J. A. Receptor tyrosine kinases and TLR/IL1Rs unexpectedly activate mye-

loid cell PI3K γ, a single convergent point promoting tumor inflammation and progression. *Cancer Cell* **2011**, *19*, 715-727.

(10) Joshi, S.; Singh, A. R.; Zulcic, M.; Durden, D. L. A macrophage-dominant PI3K isoform controls hypoxia-induced HIF1alpha and HIF2alpha stability and tumor growth, angiogenesis, and metastasis. *Mol. Cancer. Res.* **2014**, *12*, 1520-1531.

(11) Gunderson, A. J.; Kaneda, M. M.; Tsujikawa, T.; Nguygen, A. V.; Affara, N. I.; Ruffell, B.; Gorjestani, S.; Liudahl, S. M.; Truitt, M.; Olson, P.; Kim, G.; Hanahan,, D.; Tempero, M. A.; Sheppard, B.; Irving, B.; Chang, B. Y.; Varner, J. A.; Coussens, L. M. Bruton tryrosine kinase-dependent immune cell cross-talk drives pancreas cancer. *Cancer Discovery* **2016**, *6*, 270-285.

(12) Rivera, L. B.; Meyronet, D.; Hervieu, V.; Frederick, M. J.; Bergsland, E.; Bergers, G. Intratumoral myeloid cells regulate responsiveness and resistance to antiangiogenic therapy. *Cell Rep*. **2015**, *11*, 577-591.

(13) De Palma, M.; Lewis C. E. Macrophage regulation of tumor responses to anticancer therapies. *Cancer Cell*. **2013**, *23*, 277-286.

(14) Cushing, T. D.; Metz, D. P.; Whittington, D. A.; McGee, L. R. PI3Kδ and PI3Kγ as targets for autoimmune and inflammatory diseases. *J. Med Chem*. **2012**, *55*, 8559-8581.

(15) Bergamini, G.; Bell, K.; Shimamura, s.; Werner, T.; Cansfield, A.; Mueller, K.; Perrin, J.; Tau, C.; Ellard, K.; Hopf, C.; Doce, C.; Leggate, D.; Mangano, R.; Mathieson, T.; O'Mahony, A.; Plavec, I.; Rharbaoui, F.; Savitski, M. M.; Ramsden, N.; Hirsch, E.; Drewes, G.; Rausch, O.; Bantscheff, M.; Neubauer, G. A selective inhibitor reveals PI3Kγ dependence of TH17 cell differentiation. *Nat. Chem. Biol.* **2012**, *8*, 576-582.

(16) Sunose, M.; Bell, K.; Ellard, K.; Bergamini, G..; Neubauer, G.; Werner, T.; Ramsden, N. Discovery of 5-(2-amino-[1,2,4]triazolo[1,5-a]pyridin-7-yl)-N-(tert-butyl)pyridine-3-sulfonamide (CZC24758), as a potent, orally bioavailable and selective inhibitor of PI3K for the treatment of inflammatory disease. *Bioorg. Med. Chem. Lett*. **2012**, *22*, 4613-4618.

(17) Leahy, J. W.; Buhr, C. A.; Johnson, H. W. B.; Kim, B. G.; Baik, T.; Cannoy, J.; Forsyth, T. P.; Jeong, J. W.; Lee, M. S.; Ma, S.; Noson, K.; Wang, L.; Williams, M.; Nuss, J. M.; Brooks, E.; Foster, P. Goon, L.; Heald, N.; Holst, C.; Jaeger, C.; Lam, S.; Lougheed, J.; Nguyen, L.; Plonowski, A.; Song, J.; Stout, T.; Wu, X.; Yakes, M. F.; Yu, P.; Zhang, W.; Lamb, P.; Raeber, O. Discovery of a novel series of potent and orally bioavailable phosphoinositide 3-kinase γ inhibitors. *J. Med. Chem*. **2012**, *55*, 5467-5482.

(18) Roller, A.; Perino, A.; Dapavo, P.; Soro, E.; Okkenhaug, K.; Hirsch, E.; Ji, H.; Blockade of phosphatidylinositol 3-kinase (PI3K)δ or PI3Kγ reduces IL-17 and ameliorates imiquimod-induced psoriasis-like dermatitis. *J. Immunol*. **2012**, *189*, 4612-4620.

(19) Oka, Y.; Yabuuchi, T.; Oi, T.; Kuroda, S.; Fujii, Y.; Ohtake, H.; Inoue, T.; Wakahara, S.; Kimura, K.; Fujita, K.; Endo, M.; Taguchi, K.; Sekiguchi, Y. Discovery of N-{5-[3-(3-hydroxypiperdin-1-yl)-1,2,4-oxadiazol-5-yl]-4-methyl-1,3-thiazol-2-yl}acetamide (TASP0415914) as an orally potent phosphoinositide 3-kinase γ inhibitor for the treatment of inflammatory diseases. *Bioorg. Med. Chem*. **2013**, *21*, 7578-7583.

(20) Bruce, I.; Akhlaq, M.; Bloomfield, G. C.; Budd, E.; Cox, B.; Cuenoud, B.; Finan, P.; Gedeck, P.; Hatto, J.; Hayler, J. F.; Head, D.; Keller, T.; Kirman, L.; Leblanc, C.; Grand, D. L.; McCarthy, C.; O'Connor, D.; Owen, C.; Oza, M. S.; Pilgrim, G.; Press, N. E.; Sviridenko, L.; Whitehead, L. D. Development of isoform selective PI3K-kinase inhibitors as pharmacological tools for elucidating the PI3K pathway. *Bioorg. Med. Chem. Lett.* **2012**, *22*, 5445-5450.

(21) Collier, P. N.; Martinez-Botella, G.; Cornebise, M.; Cottrell, K. M.; Doran, J. D.; Griffith, J. P.; Mahajan, S.; Maltais, F.; Moody, C. S.; Huck, E. P.; Wang, T.; Aronov, A. M. Structural basis for isoform selectivity in a class of benzothiazole inhibitors of phosphoinositide 3-kinase γ. *J. Med Chem*. **2015**, *58*, 517-521.

(22) Collier, P. N.; Messersmith, D.; Le Tiran, A.; Bandarage, U. K.; Boucher, C.; Come, J.; Cottrell, K. M.; Damagnez, V.; Doran, J. D.; Griffith, J. P.; Khare-Pandit, S.; Krueger, E. B.; Ledeboer, M. W.; Ledford, B.; Liao, Y.; Mahajan, S.; Moody, C. S.; Roday, S.; Wang, T.; Xu, J.; Aronov, A. M. Discovery of highly isoform selective thiazolopiperidine inhibitors of phosphoinositide 3-kinase γ. *J. Med. Chem*. **2015**, *58*, 5684-5688.

(23) Boyd, M. J.; Aronov, A.; O'Dowd, H.; Green, J. A selective inhibitor of phosphatidylinositol 3-kinase-gamma. WO 2015/048318.

(24) Winkler, D. G.; Faia, K. L.; DiNitto, J. P.; White, K. F.; Brophy, E. E.; Ping, M. M.; Proctor, J. L.; Lussier, J.; Martin, C. M.; Hoyt, J. G.; Tillotson, B.; Murphy, E. L.; Lim, A. R.; Thomas, B. D.; MacDougall, J. R.; Ren, P.; Liu, Y.; Li, L.-S.; Jessen, K. A.; Fritz, C. C.; Dunbar, J. L.; Porter, J. R.; Rommel, C.; Palombella, V. J.; Changelian, P. S.; Kutok, J. L. PI3K-δ and PI3K-γ inhibition by IPI-145 abrogates immune responses and suppressed activity in autoimmune and inflammatory disease models. *Chem. Biol.* **2013**, *20*, 1364-1374.

(25) Knight, Z. A.; Gonzalez, B.; Feldman, M. E.; Zunder, E. R.; Goldenberg, D. D.; Williams, O.; Loewith, R.; Stokoe, D.; Balla, A.; Toth, B.; Balla, T.; Weiss, W. A.; Williams, R. L.; Shokat, K. M. A pharmacological map of the PI3-K family defines a role for p110alpha in insulin signaling. *Cell* **2006**, *125*, 733-747.

(26) Berndt, A.; Miller, S.; Williams, O.; Lee, D. D.; Houseman, B. T.; Pacold, J. I.; Gorrec, F.; Hon, W.-C.; Liu, Y.; Rommel, C.; Gaillard, P.; Ruckle, T.; Schwarz, M. K.; Shokat, K. M.; Shaw, J. P.; Williams, R. L. The p100 delta structure: mechanisms for selectivity and potency of new PI(3)K inhibitors. *Nat. Chem. Biol*. **2010**, *6*, 117-124.

(27) Reif, K.; Okkenhaug, K.; Sasaki, T.; Penninger, J. M.; Vanhaesebroeck, B.; Cyster, J. G. Cutting edge: Differential roles for phosphoinositide 3-kinases, p110γ and p110δ, in lymphocyte chemotaxis and homing. *J. Immunol*. **2004**, *173*, 2236-2240.

(28) Kutok, J.; Ali, J.; Brophy, E.; Castro, A.; DiNitto, J.; Evans, C.; Faia, K.; Goldstein, S.; Kosmider, N.; Lescarbeau, A.; Liu, T.; Martin, C.; McGovern, K.; Nair, S.; Pink, M.; Proctor, J.; Rausch, M.; Sharma, S.; Soglia, J.; Tchaicha, J.; Tremblay, M.; Villegas, V.; Walsh; White, K. Winker, D.; Palombella, V. The Potent and Selective Phosphoinositide-3-Kinase (PI3K)-γ Inhibitor, IPI-549, Inhibits Tumor Growth in Murine Syngeneic Solid Tumor Models through Alterations in the Immune Suppressive Microenvironment. In *CRI-CIMT-EATI-AACR – The Inaugural International Cancer Immunotherapy Conference: Translating Science into Survival*, New York, Sept. 16-19, 2015.

(29) NCT02637531: A dose-escalation study to evaluate the safety, tolerability, pharmacokinetics, and pharmacodynamics of IPI-549. www.clinicaltrials.gov.

FOR TABLE OF CONTENTS USE ONLY:

Compound **26** is a potent and highly selective inhibitor of PI3K-γ

Assay	PI3K Isoform			
	α	β	γ	δ
K_d (nM)	17	82	0.29	23
Biochemical IC_{50} (nM)	3200	3500	16	>8400
Cellular IC_{50} (nM)	250	240	1.2	180

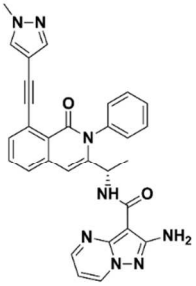

26 (IPI-549)